SLAC-PUB-12959
November, 2007

Beam-Ion Instability in PEP-II *

S. Heifets, A. Kulikov, Min-Huey Wang, U. Wienands
Stanford Linear Accelerator Center, Stanford University, Stanford, CA 94309, USA

Abstract

The instability in the PEP-II electron ring has been observed while reducing the clearing gap in the bunch train. We study the ion effects in the ring summarizing existing theories of the beam-ion interaction, comparing them with observations, and estimating effect on luminosity in the saturation regime. Considering the gap instability we suggest that the instability is triggered by the beam-ion instability, and discuss other mechanisms pertinent to the instability.

0.1 Introduction

The paper is inspired by recent observation of beam instability at PEP-II electron HER [1]. The instability took place when the ion gap was reduced below a certain minimum length for colliding beams. In the paper, we summarize the theories of the beam-ion interaction reproducing in the Appendix the main theoretical results of the different regimes of the linear theory and clarifying the limits of their applicability. We distinguish three regimes of ion instability emphasizing that experiments can not be described by the linear theories, show results of the nonlinear analysis, and estimate ion effect on luminosity in the saturation regime. We also discuss the gap instability and present arguments that the instability can be triggered by the ions in the ring and discuss other relevant effects.

0.2 Linear theories of the beam-ion interaction

The beam-ion instability is well known since the pioneering paper by Zenkevich and Koshkarev [2]. Usually it is assumed that ions are generated in collisions of the beam with the residual gas with the rate per unit length per unit time

*Work supported by US Department of Energy contract DE-AC02-76SF00515

$$S_0 = \frac{d^2 N_i}{dsdt} = \sigma_i^+ n_g N_B \frac{c}{s_b} \tag{1}$$

given in terms of the bunch population N_b, bunch spacing s_b, and the ionization cross-section σ^+. The residual gas density n_g at normal temperature is defined by the pressure P,

$$n_g = 3.2\,10^7\,\frac{P}{nTorr} \quad \mathrm{cm}^{-3}. \tag{2}$$

The cross-sections and densities of the residual gas are given in Table 1 for four main species at room temperature and pressure 1 nTorr [3]. Below, we take the usual estimate $\sigma_i = 2$ Mbarn for the cross-section averaged over partial pressure of gas species. It is worth noticing that actual gas composition is not well known because high flux of synchrotron radiation photons may dissociate molecules to single-atom species and heavy ions can be present due to damaged silver, copper, and TiN vacuum surfaces.

Table 1. Cross-sections and partial densities of the residual gas.

	A	σ_{col}, $Mbarn$	Partial P, %	n, $10^7\,cm^{-3}nTorr^{-1}$
H_2	2	0.35	75	2.4
CO	28	1.9	0.14	0.46
CO_2	44	3.0	0.07	0.22
CH_4	16	2.1	0.04	0.12

Ions interacting with the train of bunches are trapped at the beam line and oscillate with the ion frequency $\Omega^i_{x,y}$,

$$(\frac{\Omega^{(i)}_{x,y}}{c})^2 = \frac{2N_b r_p}{A\sigma_{x,y}(\sigma_x + \sigma_y)s_b}. \tag{3}$$

Here, r_p is the classical proton radius, c is velocity of light, A is ion atomic number, and $\sigma_{x,y}$ are transverse rms dimensions of the beam. Oscillations are stable provided that $\Omega^{(i)} s_b/2c < 1$. Usually, this single-turn condition is fulfilled and ions are trapped along the train. For small $\Omega^{(i)} s_b/2c << 1$, the beam can be considered as a coasting beam. It is worth noting that for new machines, with extremely small beam transverse rms such as in the Super-B factory, the one-turn stability may not take place at least for hydrogen. In this case, the average ionization cross-section would be substantially reduced as it is clear from Table 1.

If there is a gap with the length $L = cT_g$, ions may still remain multi-turn stable if

$$|\cos(\psi_{x,y} + \alpha_{x,y})| < \cos(\alpha), \tag{4}$$

where

$$\psi_{x,y} = \Omega^{(i)}_{x,y} T_0 (1 - \frac{T_g}{T_0}), \quad \sin(\alpha_{x,y}) = \frac{\Omega^{(i)}_{x,y} T_g/2}{\sqrt{1 + (\Omega^{(i)}_{x,y} T_0/2)^2}}, \tag{5}$$

and T_0 is revolution period.

These conditions of ion stability are obtained (see, for example, Appendix 1) assuming train of equidistant bunches moving with zero transverse excitation along the beam line. In the steady-state case, ions generated at the beam line accumulated until the space-charge starts driving ions toward the wall. The quasi-steady state ion distribution is derived in Appendix 2 and is shown in Fig. (1). The density on the beam line is given by the condition of neutrality $dN_i/ds = N_b/s_b$ and can be very high.

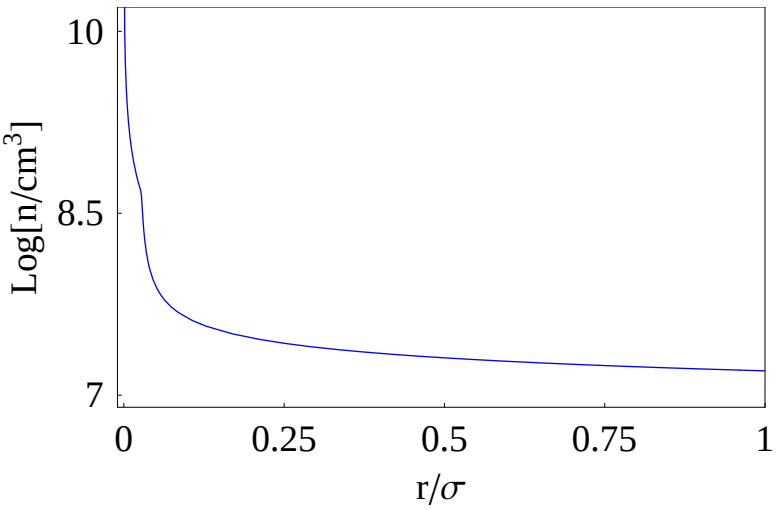

Figure 1: Density profile for round geometry. The density rolls off from $n(0) = 1.3\,10^{10}$ cm^{-3} on the beam line given by the condition of neutrality to the average density across the beam pipe $n \simeq 10^7$ cm^{-3}.

Suppose now that beam oscillates vertically with the bunch-to-bunch phase modulation $y(s,z) = a\cos(\omega_\beta s/c - \Omega z/c)$, where z, $0 < z < L$, is distance of a bunch from the head of the train and $s = ct - z$ is the bunch location. Then, at a given location s in the ring, an ion sees the field $\propto a\cos(\omega_\beta s/c - \Omega(t - s/c))$ of the bunch $z = ct - s$. The signal is modulated with frequency Ω and, if $\Omega = \Omega^{(i)}$, is in resonance with free ion oscillations increasing the amplitude of ion oscillations linearly in time. In turn, ion oscillations affect the beam. Zenkevich and Koshkarev have demonstrated that beam interacting with the residual gas ionized in collisions is unstable and the amplitudes of the beam and ions grow exponentially. The instability for a coasting beam took place (see Appendix 5.3) when the frequency of a revolution harmonic $n\omega_0$ is within the ion frequency distribution and the growth rate is maximum for the revolution harmonics $n\omega_0 = \omega_\beta + \Omega_i$ where Ω_i is linear frequency Eq. (3).

For bunch trains with a large clearing gaps, the beam-ion instability does not have resonance character. The instability in this case is the fast-ion instability (FII) discovered by T. Raubenheimer and F. Zimmermann [4] and is driven by the ions generated by the beam in one turn. Contrary to the Zenkevich-Koshkarev theory, where the ion density is a fitting given parameter, the one-turn ion density in the FII is well defined by the residual gas pressure.

The original linear theory [4] of the FII predicts the quasi-exponential growth of the amplitude a of oscillations of bunch centers $a \propto e^{\sqrt{\tau/\tau_0}}$. It is convenient to describe the beam-ion interaction in terms of the dimensionless variables

$$\tau = \frac{\omega_y s}{c}, \quad \zeta = \frac{\Omega_y^{(i)} z}{c}, \tag{6}$$

where $\omega_y = Q_y \omega_0$ and Q_y is the betatron tune. In such units, the effective FII growth rate in the vertical plane is

$$\begin{aligned} &\frac{1}{\tau_0} = \Lambda_0 \zeta^2, \\ &\Lambda_0 = \frac{2 r_e}{\gamma\, \Omega_{i,y}} \langle \frac{S_0}{\sigma_y(\sigma_x + \sigma_y)} \rangle \, (\frac{c}{\omega_y})^2. \end{aligned} \tag{7}$$

Here r_e is classical electron radius and γ is relativistic factor. We reproduce this result in the Appendix 5.1.

It is worth noting that ions in the theory of FII are described, for the cold beam, by oscillatory equation. Thus, it is implied that ions are one-turn stable what, as it was mentioned above, may be wrong for a Super-B machine. In this case, the FII would be substantially suppressed.

The next step in the theory was taken by G. Stupakov [5] who took into account the variation of the ion frequency around the ring $\epsilon = \Delta\Omega_i/\Omega_i$ due to variation of the beam rms at different locations. The growth becomes exponential $a \propto e^{\tau/\tau_S}$ (see Appendix 5.2, Eq. (78), where

$$\frac{1}{\tau_S} = \frac{\Lambda_0\, \zeta^2}{4\sqrt{2}\, \epsilon\, \zeta}, \quad (\text{for } \epsilon \simeq 0.1), \tag{8}$$

and is reduced by the factor $\epsilon\zeta >> 1$ compared to Eq. (7). Eq. (8) is applicable (see Appendix 5.2, Eq. (8)) if

$$\epsilon >> \sqrt{\frac{\Lambda_0 \tau}{2}}. \tag{9}$$

Otherwise, for $\epsilon << \sqrt{\Lambda_0 \tau/}$, the quasi-exponential result Eq. (7) is valid.

It is worth noting that usually Eq. (8) is understood with ζ taken at the tail $z = L$ of the train, $\zeta = \Omega L/c$. That is correct if the growth rate Eq. (8) is relatively small and the

amplitude of ion oscillations does not grow within the length of the train to values larger than several rms σ_y. Otherwise, such ions lose memory of the beam offset and the length of the train L has to be replaced by such length where that happens.

The growth rate in Zenkevich-Koshkarev theory (see Eq. (92), Appendix 5.3) and the growth rate Eq. (8 are given by the same expression (apart of the factor $\pi/2$) if both are written in terms of the ion density n_i. However, the density is very different being given by the ions generated in one turn for FII and is determined by the space-charge limit for multi-turn stable ions.

It would be very difficult to observe the exponential regime directly although some experiments are quite consistent with the theory [6].

D. Pestrikov [7] noticed that the build-up of ion density along the train leads to the bunch-to-bunch tune variation along the train. This effect works similar to Landau damping. Indeed, the beam becomes stable when (see Appendix 2, Eq. (51)))

$$\frac{\Lambda_0 \tau}{8} > 1. \tag{10}$$

However, Stupakov [8] noticed that condition Eq. (10) corresponds to a very large time. In reality, the beam does cease to follow the linear theory much earlier than the tune variation can take effect.

Results Eqs. (7)-(10) were obtained in the linear approximation and, for completeness, we reproduce them in Appendix 2. We refine the result of Eq. (8) and show that the Stupakov's regime has to be replaced by the original result Eq. (7) at large time. However, similar to the case of Pestrikov's regime Eq. (10), the linear theory ceased to be valid earlier than it can happen.

0.3 Linear theories in PEP-II

In the following we apply results of the linear theory to the PEP-II electron ring lattice and typical parameters: the beam current 1.75 A, the beam energy $E = 9.1$ GeV, the revolution time $T_0 = 7.3$ μs, tune $Q_y \simeq 26.5$, the typical average transverse rms $\sigma_x = 0.8$ mm, $\sigma_y = 150\,\mu m$, the beam separation $s_b/c = 4.3\,ns$, the bunch population $N_b = 4.5\,10^{10}$, and the typical base pressure $P = 2$ nTorr.

With such parameters, the production rate of ions $S_0 = 1.4\,10^9\ 1/(cm\,s)$. For ions with atomic number $A = 28$, the ion frequencies $\Omega_{i,y} \simeq 50$ MHz, $\Omega_{i,x} s_b/2c = 0.04$, $\Omega_{i,y} s_b/2c = 0.10$ and ions are one-turn stable. The exponential growth stops according to Pestrikov's theory when $\Lambda_0 \tau/8 \simeq 1$, or only after 350 ms, well beyond applicability of the linear theory. Hence, within the linear theory, only the Stupakov's regime Eq. (8) may be applicable.

The variation of the transverse rms σ_y in the PEP-II electron ring is shown in Fig. (2). The variation of the rms leads to the ion frequency variation which can be described by the parameter $p(\tau)$,

$$p^2(\tau) = (\frac{1}{\sigma_y(\sigma_x+\sigma_y)})\langle\frac{1}{\sigma_y(\sigma_x+\sigma_y)}\rangle^{-1}, \tag{11}$$

where the angular brackets mean averaging over the ring. Parameter $p(\tau)$ is depicted in Fig. (3).

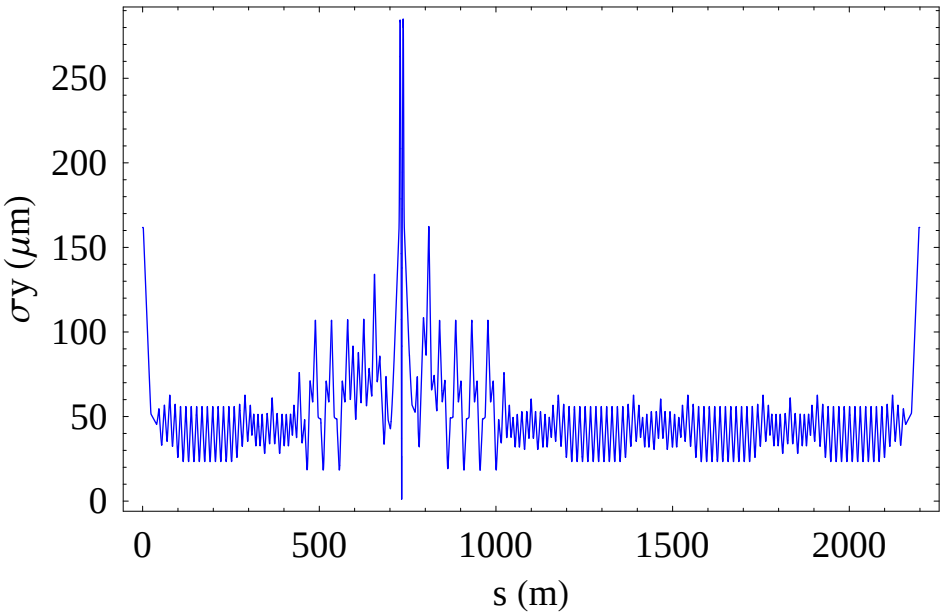

Figure 2: Variation of the rms σ_y in HER PEP-II (90^o phase advance optics).

For a periodic lattice with the period $\tau_c = 2\pi l_c\omega_\beta/c$ defined by the lattice period l_c, variation of $p(\tau)$ can be described as $p(\tau) = 1 + \epsilon\sin(\tau/\tau_s)$. Definition of the modulation amplitude ϵ for realistic lattice is given in Appendix 2. Calculations give for two PEP-II electron ring lattices values

$$\epsilon = 0.141, (90^o \text{ lattice}),$$
$$\epsilon = 0.109, (60^o \text{ lattice}).$$

With such variation, the growth time in Stupakov's theory Eq. (8) is $\tau_S = 192\,\mu s$, and beam should be unstable which seems to be in contradiction with the reality. One may argue that the beam in collision is stabilized by the beam-beam tune spread which can be as high as $\xi_{BB} = 0.1$. Indeed, the corresponding frequency spread $\delta\omega_\beta \simeq 13$ kHz can suppress the instability, see below. Dependence of a single beam stability on the gain of the transverse feeback system (TFB) deserves more careful study.

Comparing the theory and experiment we need to have in mind the following. The linear theory is applicable only as long as the amplitudes of the beam and ions are small

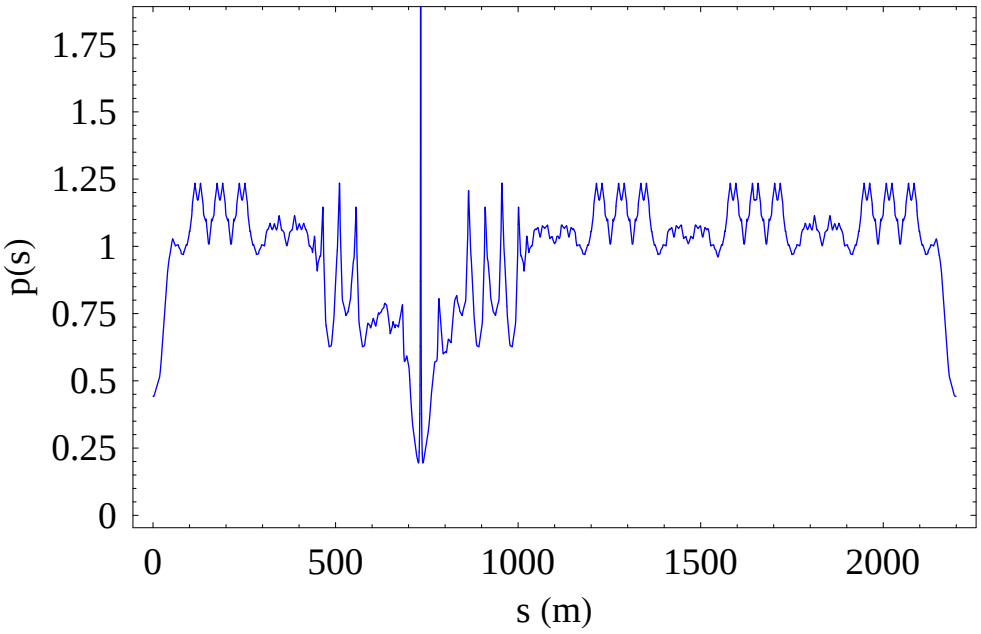

Figure 3: Parameter $p(s)$ around the ring calculated for HER PEP-II (90^o phase advance optics).

compared with the beam rms. In the linear theory, the ratio of ion to beam amplitudes is approximately given by the factor $(\Lambda\tau/\epsilon)^{-1}$. Hence, initially ion amplitude grows faster than the beam amplitude but later the relation is reverse. Limitation of small amplitudes means that the beam in observations is practically always beyond the applicability of the linear theory. The simulations [5], [9] and theory [10] show that the exponential growth is replaced by much slower growth following a power law $a \propto (\tau - \tau_0)^{1/3}$ when the beam amplitude a reaches few rms σ_y. Example of such behavior is shown in Fig. (4).

Can the ion instability affects the projected rms of the beam? The optical model, see Table 2, predicts transverse rms factor 2-3 smaller than measured.

Table 2. rms of the PEP-II HER beam at the interaction point given by the optical model

$s(m)$	σ_x (μ m, MAD)	σ_y (μ m, MAD)
733.10	128.93	1.103

Usually, a TFB has a damping rate Γ_{FB} smaller than the growth rate of instability in the initial exponential regime. The PEP-II feedback is effective for instabilities with the growth time larger than, probably, 0.1 ms. When the amplitude is large enough to start the nonlinear regime, the TFB can stop further growth. We can model the situation by the equation for the amplitude $a(\tau)$ in the form

$$\frac{da(\tau)}{d\tau} = \frac{\Gamma\, a(\tau)}{1 + \alpha\,(a(\tau)/\sigma_y)^3} - \Gamma_{FB}\, a(\tau), \tag{12}$$

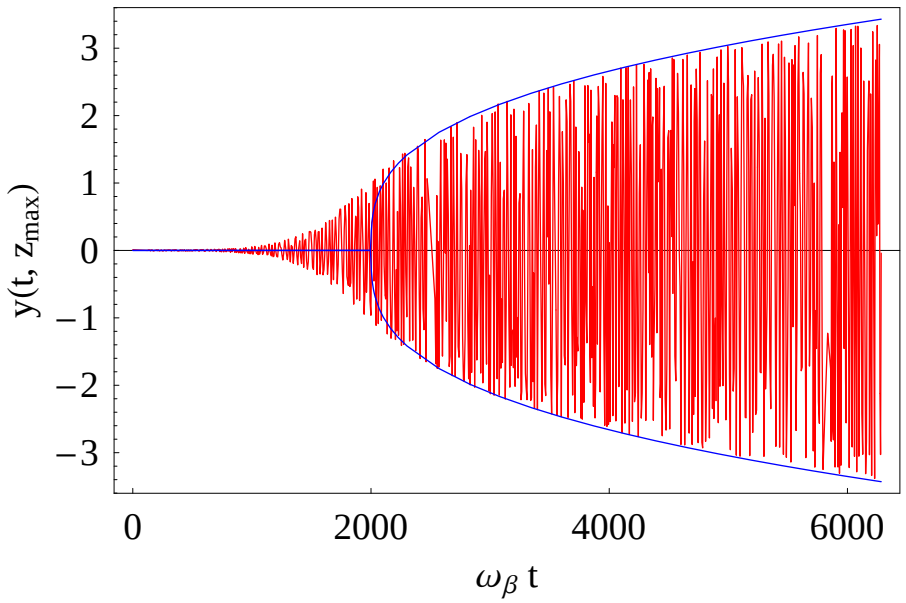

Figure 4: Nonlinear growth of instability. The power law $a \propto (\tau - \tau_0)^{1/3}$ at large $\tau > \tau_0$ replaces the initial exponential growth of the amplitude for a bunch at the tail of the train. Numerical results (red line) agrees with analytic estimate for the envelope of oscillations [10] (blue line).

where $a(0) << \sigma_y$ is the initial seed amplitude to start the instability, Γ is the growth rate of instability in the linear regime without TFB, and α is a parameter of the nonlinearity of the beam-ion interaction. Parameter α defines the amplitude $a_{sat} \simeq (2-3)\sigma_y$ at which the linear regime is replaced by the power law growth, $\alpha(a_{sat}/\sigma_y)^3 \simeq 1$. Without TFB, Eq. (12) describes initial exponential growth $a(\tau) = a(0)e^{\Gamma\tau}$ which changes to

$$a(\tau) \simeq (\frac{3\,\Gamma\,\tau}{\alpha})^{1/3}, \quad \text{for} \quad \Gamma\tau >> (1/3)\ln[\frac{3\,\Gamma\,\tau}{\alpha}\,(\frac{\sigma_y}{a(0)})^3]. \tag{13}$$

With the TFB on, the solution of Eq. (12) is shown in Fig.(5). For calculations we assume $\alpha = 0.1$, initial amplitude $a(0) = 10^{-3}$, the ratio $\Gamma_{FB}/\Gamma = 0.1$ and $\Gamma_{FB}/\Gamma = 0.2$.

The amplitude for large $\Gamma\tau$ goes to zero if $\Gamma < \Gamma_{FB}$ or to a constant value

$$a_\infty = \sigma_y\,[\frac{1}{\alpha}(\frac{\Gamma}{\Gamma_{FB}} - 1)]^{1/3}, \quad \Gamma > \Gamma_{FB}. \tag{14}$$

Effect of the beam-beam tune spread $\Delta\omega_\beta$ is equivalent to increasing TFB damping effectively replacing Γ_{FB} by $\Gamma_{FB} + \Delta\omega_\beta$. For reasonable $1/\Gamma \simeq 200\,\mu s$, $1/\Gamma_{FB} = 500\,\mu s$, and the beam can be stabilized by quite low beam-beam tune spread $\xi_{BB} = 0.005$.

The TFB defines as well the steady-state amplitude in the model where the instability saturates asymptotically in time. To illustrate that let us consider a model where the

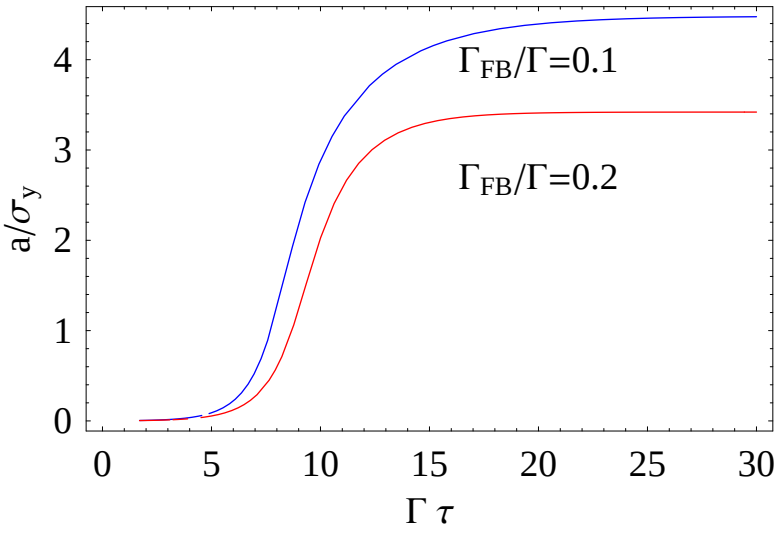

Figure 5: Saturation of the instability with the TFB turned on.

amplitude changes according to equation

$$\frac{da(t)}{dt} = \frac{a_\infty - a_0}{\tau_0}\,[1 - (\frac{a(t) - a_0}{a_\infty - a_0})^2] - g\,a(t). \tag{15}$$

Parameter g here is the damping rate introduced by the TFB, and τ_0 is the growth time of instability. If $g = 0$, the amplitude $a(t)$ growth from the initial $a(0)$ approaching the asymptotic a_∞,

$$a(t) = a_0 + (a_\infty - a_0)\,\tanh(\frac{t}{\tau_0}). \tag{16}$$

With $g > 0$, the character of growth is the same but the asymptotic value decreases as it is shown in Fig. (6). The asymptotic value of $a(t)$ in saturation is shown in Fig. (7) vs the damping rate g.

As Figs. (6)-(7) show, the steady-state amplitude remains quite noticeable even at large damping rates of the TFB system. It may explain why the rms defined in collisions from the luminosity measurements is always several times larger than predicted by the optical model.

We think that careful study of the apparent discrepancy between optical model and luminosity measurements are needed to estimate effect of other mechanisms such as parasitic dispersion at the interaction region or x/y coupling. Large saturation amplitude would reduce the luminosity causing periodic variation of a bunch offset at the collision point. Even if the amplitude in saturation is the same for all bunches, it can possibly be detected as turn-by-turn luminosity variation for a given bunch unless bunch center motion is accompanied by similar growth of the bunch transverse rms. The latter effect

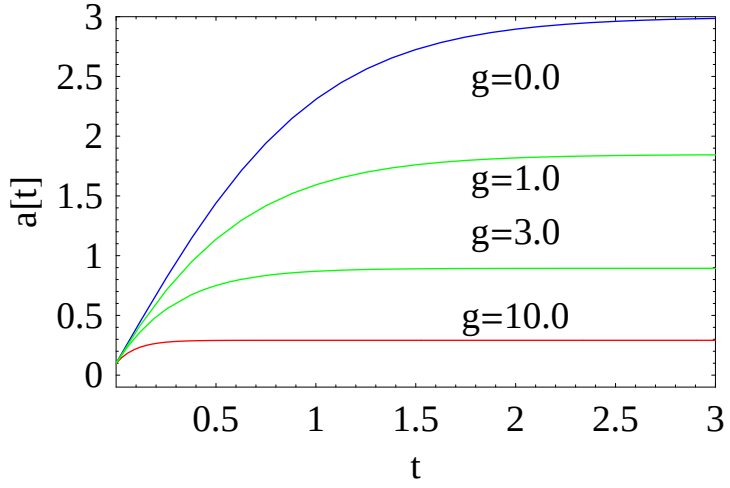

Figure 6: Variation of the $a(t)$ for a model Eq. (15) for several values of the TFB damping rate g. Parameters used $a_0 = 0.1$, $\tau_0 = 1.0$.

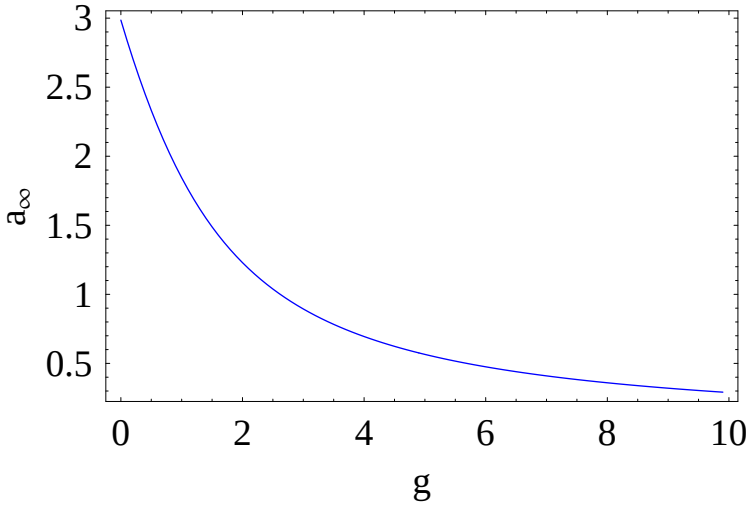

Figure 7: Asymptotic value of $a(t)$ for a model Eq. (15) vs the TFB damping parameter g. Parameters are the same as in Fig. (6).

is considered in the theory of the single-bunch electron cloud theory where dynamics of bunch slices can be substantially different. It is doubtful that such effect is noticeable for beam-ion interaction with much lower ion frequencies.

We also has to have in mind that our estimates use some parameters such as the average rms of the beam which are not very well known. The actual rms may be different from the optical model, and measurements may give only projected rms of the beam

including the centroid offset.

1 The gap instability

The FII instability assumes that ions are cleared out in one turn and instability is caused by the ions generated in one turn. The clearing gap in the train of bunches is introduced to reduce the ion density. Operation of high-current machine with a large gap, however, is difficult because the gap causes transient behavior in the rf system and along the train. For this reason, the shorter the gap the better and there was attempt to reduce the clearing gap in PEP-II [1]. In the experiment, the transient variation of the rf phase along the train, indeed, was reduced for smaller gaps. However, the beam became unstable when the gap was reduced to approximately 15 bunches. This gap instability had character of the transient phenomena starting from the head of the train and spreading toward the tail with the rate which allowed observation of the process in real time. The beam oscillates with large amplitude but the life time remains relatively good and the beam is not lost for an hour. The oscillations, however, affect the luminosity. Some of the experimental results are shown in Figs. (8). We present a preliminary discussion of the instability, more details will be reported elsewhere.

In Fig. (8) the top pane shows increase of the number of bunches in the train from 1730 bunches with the nominal bunch spacing of $2\lambda_{rf}$. The full ring with such bunch spacing has 1746 bunches. The middle pain shows that with 5 bunches added to the gap the projected vertical rms σ_y (averaged over all bunches in the beam) in the high energy electron (HER) ring started to grow. At the same time, the σ_y in the low-energy positron beam (LER) decreased. The strong beam oscillations accompanied the rms growth. The beam were in collisions and the luminosity drops as it is shown in the bottom pane of Fig. (8). The average beam currents degraded (mostly in LER) but very slowly (the time interval shown in Fig. (8) is about 2 hours). Attempts were made to change tunes to stabilize beams and, eventually, the beam was lost. Later the HER was refilled again, this time there were no collisions: the LER was empty, and the single HER beam was stable for the same number of additional bunches which caused instability of the colliding beams.

To explain the gap instability we analyzed condition Eq. (4) varying the length of the gap cT_g for a given current. We tried to show that for small gap the ion density can be substantially larger than the density of one-turn ions. Results are plotted in Fig. (9).

Fig. (9) shows that at large gaps almost all ions are unstable. In this case, the ion density is the density of ions generated in one turn and the maximum accumulated linear density is $dN_i/ds = S_0 T_0$. The production rate S_0 is defined in Eq. (1). For PEP-II parameters, $S_0 = 1.4\,10^9\ (cm\,s)^{-1}$ and $T_0 = 7.3\ \mu s$ give $dN_i/ds = 1.0\,10^4\ 1/cm$ per turn. The density of one-turn ions

$$n_i = \frac{S_0}{2\pi\sigma_y\sigma_x} \tag{17}$$

is $n_i = 1.3\,10^6\ cm^{-3}$, giving the tune shift for the last bunch (see Appendix 5.1, Eq. (57),

$$\Delta Q_y = \frac{\pi r_e}{\gamma}\,(\frac{c}{\omega_y})^2\,n_i\,Q_y, \tag{18}$$

which is small, $\Delta Q_y = 0.0030$ at PEP-II $I_b = 1.75$ A and $\sigma_{x/y} = 800/150\,\mu m$.

With small gaps, however, almost all ions become stable. In this case, the density is limited only by the space charge of accumulated ions and by the instability itself. Usually the linear density in such a case is estimated using the condition of neutrality. If the latter is understood as equality of the linear density of ions and of the beam, $dN_i/ds = N_b/s_b$, then the linear density of ions would be very large $n_i = 4.7\,10^{10}\ cm^{-3}$ for PEP-II parameters. Even if the actual density is only on the level of few percent of that given by neutrality, the linear density for small gap can be two order of magnitude larger than density for long gaps. Note that stability first starts in x-plane what may explain the difference in dynamics of the instability in x/y plains. The frequency of coherent oscillations observed in the experiment is consistent with the ion frequency. The growth rate of instability increases proportional to the density and the beam-beam tune spread which stabilized beam with large gap may become insufficient to stabilize the beam with reduced gap. Fig. (9) shows that ions are stable in both transverse planes simultaneously if $T_g/T_0 < 0.002$ and $0.012 < T_g/T_0 < 0.014$, which is in a reasonable agreement with the gap length at the onset of instability within uncertainty of the beam rms. It is interesting also to estimate the time it takes to build up such density, $t = (dN_i/ds)/S_0$. For PEP-II, $t = 0.26$ s, quite a macroscopic time for observations.

These arguments make plausible that ions trigger the gap instability. It is more complicate to explain the whole picture of instability which can be caused by several mechanisms. We see several other possible mechanisms affecting the instability.

The huge ion density at small gaps leads to the tune shift which would, certainly, kills the beam.

For large and different in x/y planes tune shifts, it is possible to hit a coupling resonance. Such a resonance does not kill the beam but can induce oscillations observed in experiment.

The time evolution of instability may be defined by the width of ion spectrum $\Delta\Omega_i$ which defines the number of revolution harmonics excited simultaneously. The instability then can be described as result of a low-Q wake field. The instability is similar then to the daisy-chain instability where the bump excitation moving from the head of the train toward the tail. At any given moment of time, the maximum amplitude has a bunch with the bunch number $n \propto t$ and the width of the bump has $\Delta n \simeq c/(\Delta\Omega_i s_b)$ bunches.

Another possibility is that ion tune shift changes the beam optics and, in particular, the dispersion D_x^* at the interaction point [11] and may lead to synchro-betatron resonances and the flip-flop beam-beam behavior.

The beam spectrum also depends on the gap. We need to remind, that for uniform fill the ion instability has a resonance character [2], see Appendix 5.3, and the strongest revolution harmonics is given by Eq. (91), $n\omega_0 = \Omega_0 + \omega_y$. Other resonance harmonic have lower growth rate and has to be within the window $\Delta\Omega$ around the strongest mode. Such a resonance can be avoided for the uniformly distributed bunches, where in the beam spectrum there are, ideally, only harmonics separated by $\Delta\omega = 2\pi/\tau_b$. For PEP-II bunch spacing $\tau_b = 4.2$ ns, such harmonics are rare, $\Delta\omega \simeq 238$ MHz. For the train with a gap T_g, each of these harmonics is surrounded by the revolution harmonics with the number of modes $\delta n\omega_0 \simeq \pi/T_g$. If the gap is small enough,

$$n\omega_0 \simeq \frac{\pi}{T_g} \geq \Omega_y, \tag{19}$$

one of the revolution harmonics can hit the resonance causing the beam instability. The amplitude of the resonance harmonics depends on the gap. However, in reality, some level of revolution harmonics is always present due to uneven fill of rf buckets or the residual coherent longitudinal motion of bunches and such an explanation seems to be unlikely.

It is not quite clear why a single electron beam seems to be stable with the same gap which triggers colliding beams instability. However, because the gap was reduced also in LER, the e-cloud instability was affected as well what may explain the difference of stability of a single and colliding beams.

The beams in HER and LER rings are modulated with ion and electron frequencies, respectively. Because the frequencies are different, the beam-beam force proportional to the relative offset of two beams at the interaction point is different for different bunches as it is illustrated in Fig. (10). That may be related to variation of the instability rate along the train.

Another possible explanation may be related to the difference in the transverse rms of a single beam and the beam in collision. In Fig. (12) we compare the small gap ion stability for two species with atomic numbers $A = 2$ and $A = 28$. Heavier ions remain stable for larger gaps. The same is true for dependence on the beam transverse rms: transition to ion stability for larger rms takes place earlier at larger gaps. However, the beam-beam blow-up is not large, indicating that the instability have different cause related to the beam-beam interaction and the ions only start the instability.

To summarize, we can consider the gap instability as a result of transition from the regime of the FII, where the ion density is the density of ions generated in one turn and the beam amplitudes are in saturation at relatively low level, to the resonance Koshkarev-Zenkevich regime were ions are stable and ion density can be larger by several order of magnitude than in the FII regime. If beams are in collisions, excitation of the electron

beam and the beam-beam interaction reduces the rms of the positron beam with overall reduction of luminosity.

However, available results on the gap instability should be considered as preliminary and more studies are needed. In particular, more accurate data are needed on dependence on the machine tune and on the TFB damping rate.

2 Conclusion

Observation of the gap instability was a starting motivation for our analysis. We summarize the existing theories of the beam-ion interaction, re-derived the main results of the theories, and apply them to the realistic parameters and lattice of PEP-II electron ring. We conclude that none of the theories based on the linear approximation can be applied to describe the observations. The best linear theory by Stupakov describes only the first few turns when the instability grows exponentially. The growth rate in this regime is higher than what can be handled by the transverse feedback. After that the growth continues following only a power law. With the TFB on, the beam amplitude saturates at the amplitude depending on the ratio of the growth rates of the instability and the TFB. For reasonable parameters, the estimated saturation level can be comparable with the beam rms. That does not necessarily contradict the measured rms which are indeed larger that predicted by the optical model of the ring but would reduce luminosity causing turn-by-turn variation of the bunch luminosity. We need to clarify the situation with new experiments and, maybe, refined theory.

The gap instability, on the other hand, seems to be related to a sharp increase of the ion density for small gaps where most of ions become stable and can be accumulated in many turns. The gap instability can be a result of transition from the regime of the FII, where the ion density is the density of ions generated in one turn and the beam amplitudes are in saturation at relatively low level, to the resonance Koshkarev-Zenkevich regime. For small clearing gaps in the bunch train, not only ion density increases, but also revolution harmonics are present which can hit the beam-ion resonance. Quantitatively such analysis agrees with observed in experiments. At the present time, we cannot exclude other mechanisms and more experiments are needed to clarify the gap instability.

3 Acknowledgement

S. H. appreciate discussions with G. Stupakov.

References

[1] U. Wienands, Private communication.

[2] D.G. Koshkarev and P.R. Zenkevich, Part. Accel.. 3, 1, (1972)

[3] Foster F. Rieke and William Prepejchal, Ionization Cross-sections of gaseous atoms and molecules for high-energy electrons and positrons, Phys. Rev. A, Vol. 6, No. 4, p. 1507-1619 (1972)

[4] T.O. Raubenheimer, F. Zimmermann, PR E52, No. 5 (1995) 5487

[5] G.V. Stupakov, Proc. Int. Worshop on Collective Effects and Impedance for B-factories, KEK Proc., 96-6 (1996) p. 243; SLAC-PUB-10377

[6] J. Byrd, A. Chao, S. Heifets, M. Minty, T. Raubenheimer, J. Seeman, G. Stupakov, J. Thomson, F. Zimmermannet.al., First observation of a fast beam ion instability, Phys. Rev. Lett. 79:79-82, 1997.

[7] D.V. Pestrikov Natural BNS dampling of the fast ion instability, PRST-accelerators and beams, V. 2, 044403, (1999)

[8] G.V.Stupakov Comment on natural BNS dampling of the fast ion instability, PRST-accelerators and beams, 3:019401, (2000)

[9] S. Heifets Saturation of the ion induced transverse blow-up instability, International Workshop on Collective Effects and Impedance for B-Factory, Tsukuba, Japan, June 1995, SLAC-95-6792, (1995), SLAC-PUB-6569, (1996).

[10] S. Heifets Asymptotic behavior of the electron cloud instability, SLAC-PUB-12538, June 2007. Presented at the ECLOUD07 Workshop, Daegu, Korea, 2007.

[11] S. Heifets, S. Novokhatski, D. Teytelman, Optical effects of the wake fields in the PEP-II SLAC B-factory, Phys.Rev.ST Accel.Beams 10:011001,2007.

4 Appendix 1. The beam-ion interaction

Interaction of the ion with a beam electron is Coulomb interaction. The field of a relativistic electron is

$$eE_y = \frac{\gamma e^2 (Y-y)}{[(Y-y)^2 + (X-x)^2 + \gamma^2 (ct)^2]^{3/2}}, \tag{20}$$

where X, Y and x, y are coordinates of an ion and the electron separated by the distance ct. Neglecting the shift of particles on the time scale $\sigma_\perp/\gamma$, the interaction can be described as a kick to the ion

$$\Delta(\frac{Y}{dt}) = \int dt \frac{eE_\perp}{Am_p} = -\frac{2r_p c}{A} \frac{Y-y}{(Y-y)^2 + (X-x)^2}. \tag{21}$$

The kick from a Gaussian bunch can be obtained convoluting Eq. (21) with the bunch transverse distribution centered at y_c, x_c. It is convenient to introduce additional integration presenting result in the form

$$\Delta(\frac{Y}{dt}) = -\frac{2r_p N_B c}{A}\,(Y - y_c)\int_0^\infty \frac{d\mu}{\sqrt{1+2\mu\sigma_x^2}(1+2\mu\sigma_y^2)^{3/2}}\, e^{-\frac{\mu(X-x_c)^2}{1+2\mu\sigma_x^2}-\frac{\mu(Y-y_c)^2}{1+2\mu\sigma_y^2}}. \qquad (22)$$

In the linear approximation, exponent can be replaced by one. Then, carrying out the integration, one get

$$\Delta(\frac{Y}{dt}) = -\lambda_0\,(Y - y_c),$$
$$\lambda_0 = \frac{2r_p N_B c}{A\sigma_y(\sigma_x+\sigma_y)}. \qquad (23)$$

Interaction of the beam with an ion in the zero approximation can be considered neglecting the transverse motion of the bunches. In this case, the ion motion is defined by a series of kicks separated in time by s_b/c and free motion in between. Considering the transform of $(Y, \dot{Y})$, it is easy to see that the ion is stable provided the kick is not too large

$$\frac{\lambda_0 s_b}{4} < 1. \qquad (24)$$

The phase advance per kick ν is related to λ_0,

$$\cos\nu = 1 - \frac{\lambda_0 s_b}{2}. \qquad (25)$$

For small $\nu << 1$, the motion of an ion can be described approximately as oscillations with frequency Ω_y, defined by the phase advance $\nu = \Omega_y s_b/c$, or

$$(\frac{\Omega_y}{c})^2 = \frac{2r_p N_B\, c}{A\sigma_y(\sigma_x+\sigma_y)s_b}. \qquad (26)$$

The condition of ion stability takes the form $\Omega_y s_b/2c < 1$.

The kick from an ion to a bunch electron can be defined from Eq. (23) using the Newton's law $\gamma m_e \Delta\dot{y} = -m_p A\Delta\dot{Y}$. The kick per unit length ds to an electron of a bunch z is given by multiplying $\Delta\dot{y}$ by the number of ions generated by the previous bunches of the beam $dN_i = \sigma_i^+ n_g N_B(z/s_b)ds$. Equation of motion for a bunch in the linear approximation takes the form

$$\frac{d^2y(\tau,\zeta)}{ds^2} + (\frac{\omega_y}{c})^2\, y(\tau,\zeta) = \frac{2r_p N_B}{A\sigma_y(\sigma_x+\sigma_y)}\,\sigma_i^+ n_g N_B \int_0^z \frac{dz'}{s_b}[Y(s,z,z') - y(s,z)]. \qquad (27)$$

5 Appendix 2. Ion distribution

The ion density varies across the beam-pipe by several order of magnitude. Here we derive the ion distribution in a quasi-static approximation where ions are generated by the beam with a constant rate S_0 per unit time and unit length and are driven to the wall by the space-charge of accumulated ions. For simplicity, we consider a round beam with uniform density within the cross-section $\pi\sigma^2$ and the round beam pipe with the radius b.

In a steady-state regime, the local ion density $n(r)$ is independent of time. The continuity equation defines the ion current to the wall which has only radial component $j(r) = v(r)n(r)$,

$$v(r)n(r) = \frac{S_0}{2\pi b}\{\Theta(r-\sigma)(\frac{b}{r}) + \Theta(\sigma - r)(\frac{b}{\sigma})^2\frac{r}{b}\}, \tag{28}$$

where Θ is a step-function. The ion energy is defined by the initial conditions and remains constant while ion moves toward the wall. That defines the local velocity $v(r)$. If an ion is generated at $r = 0$ with the zero velocity, then

$$\frac{M_i v^2(r)}{2} + U(r) = U(0), \tag{29}$$

where M_i is the ion mass, and $U(r) = U_b(r) + U_{sc}(r)$ is total potential given by the sum of the space-charge potential of ions U_{sc} and the beam potential $U_b(r)$.

Finally, the Poisson equation defines U_{sc},

$$\frac{1}{r}\frac{\partial}{\partial r}r\frac{\partial U_{sc}}{\partial r} = -4\pi e^2 n(r). \tag{30}$$

It is convenient to use the dimensionless $x = r/b$, $x_m = \sigma/b$, and normalize potentials

$$\begin{aligned} &U_{sc}(r) = \frac{N_b e^2}{s_b}u_{sc}(x), \quad U_b(r) = \frac{N_b e^2}{s_b}u_b(x), \\ &u_b(x) = -\Theta(x - x_m)\,\ln(\frac{1}{x^2}) + \Theta(x_m - x)[1 - \frac{x^2}{x_m^2} + \ln\frac{1}{x_m^2}]\}. \end{aligned} \tag{31}$$

Then, combining equations, we get for $v(x) = u_{sc}(x) - u_{sc}(0)$ equation

$$\frac{\partial}{\partial x}x\frac{\partial v(x)}{\partial x} = -\frac{\Lambda}{\sqrt{u_b(x) - u_b(0) - v(x)}}\{\Theta(x - x_m) + \Theta(x_m - x)\frac{x^2}{x_m^2}\}. \tag{32}$$

Here,

$$\Lambda = S_0\,\frac{2bs_b}{N_b c}\sqrt{\frac{A_i s_b}{2N_b r_p}}, \tag{33}$$

and A_i is ion atomic number.

Eq. (32) has to be solved with initial conditions $v_(0) = 0$ and $v'(0) = 0$.

Let us consider the limit $x- > 0$. Then, substituting $v(x) \simeq -\kappa x^2/2$ in Eq. (32), we get

$$2x\kappa = \frac{\Lambda}{\sqrt{\kappa x^2/2 - x^2/x_m^2}} \frac{x^2}{x_m^2}, \tag{34}$$

or

$$\kappa\sqrt{\kappa/2 - 1/x_m^2} = \frac{\Lambda}{x_m^2}. \tag{35}$$

Usually, parameter $\Lambda x_m^2 << 1$. In this case,

$$\kappa \simeq \frac{2}{x_m^2} + (\frac{\Lambda}{2})^2. \tag{36}$$

The density $n(x)$ is given in terms of $v(r)$ by

$$n(x) = \frac{N_b}{4\pi s_b b^2} \frac{\Lambda}{x\sqrt{u_b(x) - u_b(0) - v(x)}} \{\Theta(x - x_m) + \Theta(x_m - x)\frac{x^2}{x_m^2}\}. \tag{37}$$

In particular, on the beam line, Eq. (36) gives

$$n(0) = \frac{N_b}{4\pi s_b b^2}\,\kappa = \frac{N_b}{2\pi s_b \sigma^2} \tag{38}$$

what coincide with the condition of neutrality.

The density profile can be obtained solving Eq. (32) numerically. Result is shown in Fig. (1) for PEP-II parameters $N_b = 4.5\,10^{10}$, $A_i = 28$, $b = 3$ cm, $s_b = 126$ cm, $S_0 = 1.4\,10^9\ 1/(cms)$. In this case, $x_m = 0.026$, and $\Lambda = 17.4$.

In derivation above, all ions were generated at $r = 0$. It is not difficult to show that the sane result gives assumption of ions generated uniformly at $r < \sigma$.

6 Appendix 3. Linear regime of instability

Here we reproduce the main results of the linear theory of the beam-ion instability. In the dimensionless variables τ, ζ, Eq. (27) and similar equation for ions take the form

$$\begin{aligned}
&\frac{\partial^2 Y(\tau,\zeta,\zeta')}{\partial\zeta^2} + p^2(\tau)Y(\tau,\zeta,\zeta') = p^2(\tau)y(\tau,\zeta),\\
&\frac{d^2 y(\tau,\zeta)}{d\tau^2} + y(\tau,\zeta) = \Lambda_0 p^2(\tau)\int_0^\zeta d\zeta'[Y(\tau,\zeta,\zeta') - y(\tau,\zeta)].
\end{aligned} \tag{39}$$

Solution for ions generated by the bunch z' with the zero initial velocity is

$$Y(\tau,\zeta,\zeta') = y(\tau,\zeta')\cos[(\zeta-\zeta')p(\tau)] + p(\tau)\int_0^\zeta d\zeta' \sin[(\zeta-\zeta')p(\tau)]y(\tau,\zeta'). \quad (40)$$

Substituting this result in the LHS of equation for y and integrating by parts, one gets

$$\frac{\partial^2 y(\tau,\zeta)}{\partial\tau^2} + y(\tau,\zeta) = -\Lambda_0 p^2(\tau)\int_0^\zeta \zeta' d\zeta' \cos[(\zeta-\zeta')p(\tau)]\frac{\partial y(\tau,\zeta')}{\partial\zeta'}. \quad (41)$$

For the first bunch in the train we assume unperturbed motion $y(\tau,0) = y_0\cos(\tau)$. Let us introduce slow over τ amplitude $a(\tau,\zeta)$,

$$y(\tau,\zeta) = a(\tau,\zeta)\, e^{i\tau} + c.c. \quad (42)$$

Neglecting $\partial^2 a/\partial^2\tau << \partial a/\partial\tau$, we get averaging over τ

$$\frac{\partial a(\tau,\zeta)}{\partial\tau}) = \frac{i\Lambda_0}{2}\int_0^\zeta \zeta' d\zeta' K(\zeta-\zeta')\frac{\partial a(\tau,\zeta')}{\partial\zeta'}, \quad (43)$$

with the initial condition $a(\tau,0) = y_0/2$ and, for small τ, $a(\tau,\zeta) = (y_0/2)e^{-i\zeta}$. The kernel is given by averaging over τ,

$$K(\zeta-\zeta') = \langle p^2(\tau)\,\cos[(\zeta-\zeta')p(\tau)]\rangle, \quad (44)$$

where the angular brackets denote averaging over the ring.
Laplace transform over τ

$$a(\tau,\zeta) = \int \frac{d\kappa}{2\pi i} e^{\kappa\tau}\tilde{a}(\kappa,\zeta), \quad (45)$$

gives

$$\tilde{a}(\kappa,\zeta) = \frac{a(0,\zeta)}{\kappa} + \frac{i\Lambda_0}{2\kappa}\int_0^\zeta \zeta' d\zeta' K(\zeta-\zeta')\frac{\partial\tilde{a}(\kappa,\zeta')}{\partial\zeta'}. \quad (46)$$

The boundary condition takes the form

$$\tilde{a}(\kappa,0) = \frac{y_0}{2\kappa}. \quad (47)$$

6.1 FII neglecting ion frequency spread

First, we neglect the variation of ion frequency taking $p(\tau) = 1$ and $K(\zeta-\zeta') = \cos(\zeta-\zeta')$. For such a simple kernel, Eq. (46) can be reduced to a differential equation by differentiating it twice over ζ,

$$(1-\frac{i\Lambda_0}{2\kappa}\zeta)\frac{\partial^2\tilde{a}(\kappa,\zeta)}{\partial^2\zeta} - \frac{i\Lambda_0}{2\kappa}\frac{\partial\tilde{a}(\kappa,\zeta)}{\partial\zeta} + \tilde{a}(\kappa,\zeta) = \frac{a(0,\zeta)}{\kappa} + \frac{\partial^2}{\partial\zeta^2}(\frac{a(0,\zeta)}{\kappa}). \quad (48)$$

Solution of Eq. (46) is given by the superposition of the Bessel functions

$$\tilde{a}(\kappa,\zeta) = c_1(\kappa) I_0(\frac{2}{\alpha}\sqrt{1-i\alpha\zeta}) + c_2 K_0(\frac{2}{\alpha}\sqrt{1-i\alpha\zeta}), \quad \alpha = \frac{\Lambda_0}{2\kappa}. \tag{49}$$

Initial condition Eq. (47) can be satisfied using identity $I_1(z)K_0(z)+I_0(z)K_1(z) = 1/z$ with the coefficients c_1, c_2 proportional to $K_1(2/\alpha)$ and $I_1(2/\alpha)$, respectively. The inverse Laplace transform gives after changing $\tau -> \Lambda_0\tau/4$

$$a(\tau,\zeta) = \frac{y_0}{2}\int \frac{d\kappa}{2\pi i}\, e^{\frac{\Lambda_0\kappa\tau}{4}} [K_1(\kappa) I_0(\sqrt{\kappa(\kappa-2i\zeta)}) + I_1(\kappa) K_0(\sqrt{\kappa(\kappa-2i\zeta)})]. \tag{50}$$

Changing variable $\kappa \to (\kappa+i)\zeta$, we can write Eq. (50) in the form

$$a(\tau,\zeta) = \frac{y_0}{2}\int \frac{d\kappa}{2\pi i}\, e^{\lambda\zeta(\kappa+i)} [K_1(\zeta(\kappa+i)) I_0(\zeta\sqrt{\kappa^2+1}) + I_1(\zeta(\kappa+i)) K_0(\zeta\sqrt{\kappa^2+1})], \tag{51}$$

where $\lambda = \Lambda_0\tau/4$.

The contour of integration here is along the imaginary axes in the right half κ-plane. Expression in the square brackets is proportional to $1/\kappa$ at large $|\kappa| \to \infty$. Hence, the contour can be shifted to $Re(\kappa) \to -\infty$ where the integral gives a constant. The main contribution to the integral is given by the pole at $\kappa = 0$ in the first term in the square brackets and the cut in κ-plane from $\kappa = -i$ to $\kappa = i$ in the second term. The contribution of the pole at $\zeta = -i$ reproduces the initial condition for $a(\tau, 0)$. The asymptotic therefore is defined by the cut.

The result can be obtained in a simple way using the saddle-point method. In the asymptotic $|\zeta(\kappa+i)| >> 1$, $|\zeta\sqrt{\kappa^2+1}| >> 1$, the integral

$$a(\tau,\zeta) = \frac{y_0}{4\zeta}\int \frac{d\kappa}{2\pi i}\, \frac{1}{(\kappa^2+1)^{1/4}\sqrt{(\kappa+i)}} [e^{i(1+\lambda)\zeta+\zeta\Psi_1} + e^{-i(1-\lambda)\zeta+\zeta\Psi_2}], \tag{52}$$

where

$$\Psi_{1,2}(\kappa) = \pm(1\pm\lambda)\kappa \mp \sqrt{\kappa^2+1}. \tag{53}$$

The saddle points $\kappa_\pm$ for Ψ_2 are

$$\kappa_\pm = \pm\frac{1-\lambda}{\sqrt{1-(1-\lambda)^2}}, \quad \sqrt{\kappa_\pm^2+1} = \frac{1}{\sqrt{1-(1-\lambda)^2}}, \tag{54}$$

and $\Psi_2(\kappa_+) = \sqrt{1-(1-\lambda)^2}$. It is easy to see that $1-(1-\lambda)^2 > 0$ for $0 < \lambda < 2$. Therefore, for such λ, the second term in Eq. (52) gives exponentially growing

$$a(\tau,\zeta) \propto e^{\zeta\sqrt{1-(1-\lambda)^2}}. \tag{55}$$

The saddle points for Ψ_+ can be obtained changing $\lambda \to -\lambda$. It is easy to see that $1-(1+\lambda)^2 < 0$ for all real λ. Therefore, the term $\propto e^{\Psi_1}$ gives only oscillatory terms.

For small $\lambda << 1$, Eq. (55) gives

$$a(\tau,\zeta) = \frac{y_0}{2}\,\frac{1}{2i\sqrt{\pi}}\,(\frac{1}{2\Lambda_0\tau\zeta^2})\,e^{-i\zeta(1-\lambda)+\zeta\sqrt{\frac{\Lambda_0\tau}{2}}} \tag{56}$$

reproducing the main original result [4]. Note that the solution oscillates over ζ as $e^{-i\zeta}$ what corresponds to initial $y(\tau,\zeta) \propto \cos(\tau-\zeta)$ used in [4]. The saddle-point method is applicable if $\zeta\kappa_+ >> 1$, i.e. for large $\zeta\sqrt{\Lambda_0\tau} >> 1$.

The factor $e^{i\lambda\zeta}$ increases tune by

$$\Delta Q_y = \frac{\Lambda_0}{4}\,\frac{\Omega z}{c}\,Q_y = \frac{\pi r_e}{\gamma}\,(\frac{c}{\omega_y})^2\,n_i\,Q_y. \tag{57}$$

The growth of Eq. (56) is limited by the condition $\lambda < 2$. For larger τ,

$$\frac{\Lambda_0\tau}{8} > 1, \tag{58}$$

the exponential growth is suppressed although the saddle-point method is still valid. This result has been obtained by Pestrikov [7] and interpreted as Landau damping due to tune variation along the train caused by increasing density of generated ions. Actually, the large detuning changes dependence on ζ in this regime from $e^{i\tau-i\zeta}$ at small $\lambda << 1$ to $e^{i\tau-i(1-\lambda)\zeta}$. Hence, for $\lambda > 2$ the backward wave is transformed to the forward wave what stops the growth of instability.

As it was pointed out by Stupakov [8], Pestrikov's regime for real parameters corresponds to very large τ. For example, for PEP-II electron ring, parameter $\Lambda_0\kappa\tau/8 \simeq 2.2\,10^{-5} \times$ number of turns, and the exponential growth stops by Pestrikov only after 350 ms. Much earlier, the growth is changed by the nonlinearity of interaction as it is discussed later.

6.2 FII with the ion frequency spread

Let us now restrict consideration to small $\Lambda_0\tau << 1$ but take into account the variation of the ion frequency along the ring. In this case, we can take out the fast oscillations in ζ explicitly defining the slow amplitude $A(\tau,\zeta)$ of both variables,

$$a(\tau,\zeta) = A(\tau,\zeta)\,e^{-i\zeta}. \tag{59}$$

Eq. (43) takes the form

$$\frac{\partial A(\tau,\zeta)}{\partial\tau} = \frac{i\Lambda_0}{2}\,\int_0^\zeta \zeta' d\zeta' K(\zeta-\zeta')\,e^{i(\zeta-\zeta')}\,[\frac{\partial A(\tau,\zeta')}{\partial\zeta'} - iA(\tau,\zeta')]. \tag{60}$$

Neglecting the term $\partial A/\partial\zeta' << A(\tau,\zeta)$, we get

$$\frac{\partial A(\tau,\zeta)}{\partial \tau}) = \frac{\Lambda_0}{2}\int_0^\zeta \zeta' d\zeta' A(\tau,\zeta')\, K(\zeta-\zeta')\, e^{i(\zeta-\zeta')}, \tag{61}$$

where the kernel $K(\zeta-\zeta')$ depends on $p(\tau) = 1 + \Delta p(\tau)$,

$$K(\zeta-\zeta')\, e^{i(\zeta-\zeta')} = \frac{1}{2}\,\langle p^2(\tau)\,[e^{-i\Delta p(\tau)(\zeta-\zeta')} + e^{\Delta p(\tau)(\zeta-\zeta')+2i(\zeta-\zeta')}]\rangle. \tag{62}$$

For small $\Delta p(\tau)$, the factor p^2 can be replaced by one and the second term describing fast oscillations can be neglected. That transforms Eq. (61) to

$$\frac{\partial A(\tau,\zeta)}{\partial \tau} = \frac{\Lambda_0}{4}\int_0^\zeta \zeta' d\zeta' A(\tau,\zeta')\,\langle e^{-i\Delta p(\tau)(\zeta-\zeta')}\rangle. \tag{63}$$

Let us check Eq. (63) for $\Delta p(\tau) = 0$. In this case, it can be written as the differential equation

$$\frac{\partial^2 A(\tau,\zeta)}{\partial\tau\,\partial\zeta} = \frac{\Lambda_0}{4}\,\zeta A(\tau,\zeta) \tag{64}$$

which has exact solution in the form $A(\tau,\zeta) = f(x)$, where $x = \tau\zeta^2$ and $f(x)$ is a superposition of the Bessel functions $K_0(\sqrt{\frac{\Lambda_0}{4}\,x})$ and $I_0(\sqrt{\frac{\Lambda_0}{4}\,x})$. This result agrees with Eq. (56).

For a finite Δp, it is convenient to use Laplace transform over the variable ζ. The Laplace transform $\tilde{A}(\tau,q)$ satisfies

$$\frac{\partial \tilde{A}(\tau,q)}{\partial\tau} = -\frac{\Lambda_0}{4}\,\langle\frac{1}{q+i\Delta p(\tau)}\rangle\,\frac{\partial\tilde{A}(\tau,q)}{\partial q}. \tag{65}$$

Let us consider a simple model $\Delta p = \epsilon\sin(\mu\tau)$, where $\epsilon << 1$ and μ is defined by the period of variation of the ion frequency Ω_y.(For a FODO cells, $\mu = 2\pi/\mu_0$, i.e. is inversely proportional to the phase advance per cell μ_0.) Then,

$$\langle\frac{1}{q+i\Delta p}\rangle = \langle\frac{q}{q^2+(\Delta p)^2}\rangle = \frac{1}{\sqrt{q^2+\epsilon^2}}, \tag{66}$$

and Eq. (65) takes the form

$$\frac{\partial\tilde{A}(\tau,q)}{\partial\tau} + \frac{\Lambda_0}{4\sqrt{q^2+\epsilon^2}}\,\frac{\partial\tilde{A}(\tau,q)}{\partial q} = 0. \tag{67}$$

Eq. (66) can be used to define ϵ for a realistic lattice calculating $\langle q/(q^2+(\Delta p)^2)\rangle$ for several q and approximating results by $1/(\sqrt{q^2+\epsilon^2})$.

Solution of Eq. (67) is given by an arbitrary function F,

$$\tilde{A}(\tau,q) = F[\frac{\Lambda_0\tau}{2} - q\sqrt{q^2+\epsilon^2} - \epsilon^2\ln(q+\sqrt{q^2+\epsilon^2})]. \tag{68}$$

Inverse Laplace transform gives $A(\tau,\zeta)$,

$$A(\tau,\zeta)=\int_{-i\infty}^{i\infty}\frac{dq}{2\pi i}e^{\epsilon\zeta q}F[\frac{\Lambda_0\tau}{2\epsilon^2}-q\sqrt{q^2+1}-\ln(q+\sqrt{q^2+1})+\ln\frac{1}{\epsilon}]. \tag{69}$$

We can choose F to satisfy the boundary condition $A(\tau,0)=y_0/2$. The simplest way to do that is to choose $F(x)\propto 1/x$,

$$A(\tau,\zeta)=y_0\int_{-i\infty}^{i\infty}\frac{dq}{2\pi i}\frac{\sqrt{q^2+1}\,e^{\epsilon\zeta q}}{q\sqrt{q^2+1}+\ln(q+\sqrt{q^2+1})-\ln(\frac{1}{\epsilon})-\nu^2}, \tag{70}$$

where

$$\nu^2=\frac{\Lambda_0\tau}{2\epsilon^2}. \tag{71}$$

The numerator in Eq. (70) is chosen to cancel the residue of the denominator.

Small ϵ corresponds to large ν and q. Eq. (70) can be simplified, approximately, as

$$A(\tau,\zeta)=y_0\int_{-i\infty}^{i\infty}\frac{dq}{2\pi i}\frac{q\,e^{\epsilon\zeta q}}{q^2-\nu^2}, \tag{72}$$

giving

$$A(\tau,\zeta)=y_0\cosh(\epsilon\zeta\nu)\simeq\frac{y_0}{2}\,e^{\zeta\sqrt{\Lambda_0\tau/2}}. \tag{73}$$

This result agrees with Eq. (56) obtained with $\epsilon=0$. The main contribution to the integral Eq. (70) is due to $q\simeq\nu$. The result is obtained assuming $q>>1$ and is applicable if $\nu>>1$ or

$$\epsilon<<\sqrt{\frac{\Lambda_0\tau}{2}}. \tag{74}$$

At large ϵ, ν is small and the singularity of the denominator in Eq. (70) is close to the solution q_0 of the equation

$$q_0\sqrt{q_0^2+1}+\ln(q_0+\sqrt{q_0^2+1})-\ln(\frac{1}{\epsilon})=0. \tag{75}$$

The root $q_0(\epsilon)\simeq 1$ is real and plotted in Fig.(12).

The denominator in Eq. (70) where $q=q_0+\delta$ can be expanded over δ and is equal to $2\delta\sqrt{q_0^2+1}-\nu^2$. The integration in Eq. (70) gives

$$A(\tau,\zeta)=\frac{y_0}{2}\,e^{\epsilon\zeta q_0}\,e^{\epsilon\zeta\delta}, \tag{76}$$

where

$$\delta = \frac{\nu^2}{2\sqrt{q_0^2+1}}. \tag{77}$$

The time depending factor in Eq. (76)

$$A(\tau,\zeta) \propto= \frac{y_0}{2}\, e^{\epsilon\zeta q_0}\, e^{\frac{\Lambda_0\tau\zeta}{4\epsilon\sqrt{q_0^2+1}}} \tag{78}$$

reproduces Stupakov's result [5]. Result Eq. (78) is obtained assuming $\delta < 1$, and is applicable for

$$\epsilon^2 >> \frac{\Lambda_0\tau}{\sqrt{q_0^2+1}}. \tag{79}$$

Note that condition Eq. (79) is opposite to the condition Eq. (74).

6.3 Ions in a uniformly filled ring

If a train of bunches does not have a clearing gap or the gap is small, ions are accumulated continuously and, even for a small gap, the first bunch in the train couples with the last one. Such beam is unstable and the instability has a resonance character. The ion density n_i is considered as a given constant parameter being limited by the space-charge of accumulated ions and by instability induced ion drift.

We consider a uniformly filled ring following [2]. In terms of the variables time t, location of a bunch in a train $z > 0$, and location of a bunch in the ring $s = ct - z$, Eqs. (39) take the form

$$\begin{aligned}
&\frac{\partial^2 Y(s,t,t_0)}{\partial t^2} + \Omega^2 Y(s,t,t_0) = \Omega^2[y(\hat{s},ct-s) - Y(s,t,t_0)],\\
&\frac{d^2 y(s,z)}{ds^2} + (\frac{\omega_y}{c})^2\, y(s,z) = \frac{4\pi r_e}{\gamma} n_i[Y(\hat{s},\frac{s+z}{c}) - y(s,z)],
\end{aligned} \tag{80}$$

where $\hat{s} = s\ mod(C)$, C is the ring circumference, $C = 2\pi c/\omega_0$, and t_0 is the moment when the ion was generated. We consider below the growth of instability neglecting initial conditions and drop dependence on t_0. Eqs. (80) can be simplified neglecting corrections to ion frequency Ω in the first equation and to the tune shift in the second equation retaining only the driving terms. We also take into account that ions have a frequency spread described by a normalized distribution function $\rho(\Omega)$, $\int d\Omega\rho(\Omega) = 1$, and indicate Ω by the index $Y_\Omega(t)$. Eqs. (80) take the form

$$\frac{\partial^2 Y_\Omega(s,t,t_0)}{\partial t^2} + \Omega^2 Y_\Omega(s,t,t_0) = \Omega^2 y(\hat{s},ct-s),$$

$$\frac{d^2y(s,z)}{ds^2} + (\frac{\omega_y}{c})^2\, y(s,z) = \frac{4\pi r_e}{\gamma} n_i \int d\rho(\Omega) Y_\Omega(\hat{s}, \frac{s+z}{c}). \tag{81}$$

For the uniform fill, $Y_\Omega(s,t)$ has to be periodic for a fixed t, $Y_\Omega(s+C,t) = Y_\Omega(s,t)$. Hence,

$$Y_\Omega(s,t) = \sum_{m=-\infty}^{\infty} B_m^\Omega(t)\, e^{im\omega_0 s/c - i\Omega t}, \tag{82}$$

where $B_m^\Omega(t)$ are harmonic amplitudes. Similarly, $y(s,z)$ has to be periodic for a fixed time $t = (s+z)/c$. Introducing amplitudes $b_m(t)$, we can write

$$y(s,z) = \sum_{m=-\infty}^{\infty} b_m(\frac{s+z}{c})\, e^{-im\frac{\omega_0 s}{c} - i\frac{\omega_y(s+z)}{c}}. \tag{83}$$

Eqs. (82),(83) give the driven solution for ions,

$$Y_\Omega(s,t) = \Omega \int_{t_0}^{t} dt' \sin[\Omega(t-t')] y(\hat{s}, ct' - s). \tag{84}$$

Let us look for the solution in the form

$$b_n(t) = \alpha_n e^{\mu_n t}, \quad \mu_n = i\mu_n' + \Gamma_n, \tag{85}$$

where $\alpha_n = const$, Γ_n is the growth rate, and μ_n' is the frequency shift.
Then,

$$Y_\Omega(s,t) = \Omega^2 \sum_n \frac{\alpha_n}{\Omega^2 - (\omega_y + i\mu_n)^2}\, e^{-i\frac{n\omega_0 s}{c} + (\mu_n - i\omega_y)t}. \tag{86}$$

Substituting Eqs. (86) into the second of Eqs.(81) we get the dispersion equation for μ_n,

$$[\mu_n - i(\omega_y + n\omega_0)]^2 + \omega_y^2 = \frac{4\pi r_e c^2}{\gamma} n_i \int \frac{\Omega^2 d\Omega \rho(\Omega)}{\Omega^2 - (\omega_y + i\mu_n)^2}. \tag{87}$$

If $\Gamma_n << \omega_0$, the frequency shift can be determined neglecting the right-hand-side here,

$$\mu_n' = n\omega_0 + \omega_y \pm \omega_y. \tag{88}$$

The growth rate Γ_n can be approximately determined for small Γ_n replacing the integral in Eq. (87) as

$$\int \frac{\Omega^2 d\Omega \rho(\Omega)}{\Omega^2 - (\omega_y + i\mu_n)^2} =$$
$$P.V. \int \frac{\Omega^2 d\Omega \rho(\Omega)}{\Omega^2 - (\omega_y - \mu_n')^2} + \frac{i\pi}{2} \int \Omega d\Omega \rho(\Omega) \left[\delta(\Omega - \omega_y + \mu_n') - \delta(\Omega + \omega_y - \mu_n')\right], \tag{89}$$

where *P.V.* in the first term denotes the principal value. Then, using Eq. (88),

$$\Gamma_n = \mp \frac{2\pi^2 r_e c^2}{\gamma} n_i \frac{n\omega_0 \pm \omega_y}{\omega_y} \rho(|n\omega_0 \pm \omega_y|). \tag{90}$$

The distribution $\rho(\Omega)$ is centered at $\Omega = \Omega_0$, where Ω_0 is the frequency of an ion oscillating with the zero amplitude. Therefore, the growth rate $\Gamma_n > 0$ for $n > 0$ for the resonance revolution harmonics

$$n\omega_0 = \mp\Omega_0 + \omega_y. \tag{91}$$

.

$\rho(\Omega)$ has a long tail for $\Omega < \Omega_0$ corresponding to ions with large amplitudes and is nonzero for $\Omega > \Omega_0$ due to variation of the beam rms $\sigma_{x,y}$ around the ring. The total bandwidth can be estimated as $\Delta\Omega/\Omega_0 \simeq 0.1$, and the maximum value $\rho(\Omega_0) \simeq 1/\Delta\Omega$. The growth $\Gamma_n > 0$ corresponds to the positive sign, giving the maximum growth rate

$$\Gamma_n = \frac{2\pi^2 r_e c^2}{\gamma\omega_y} \left(\frac{\Omega}{\Delta\Omega}\right) n_i. \tag{92}$$

The growth rate Eq. (92) is the same as given by Eq. (8) of the FII instability if the saturation ion density n_i is used instead of

$$\frac{S_0 t_\infty}{2\pi\sigma_x\sigma_y}. \tag{93}$$

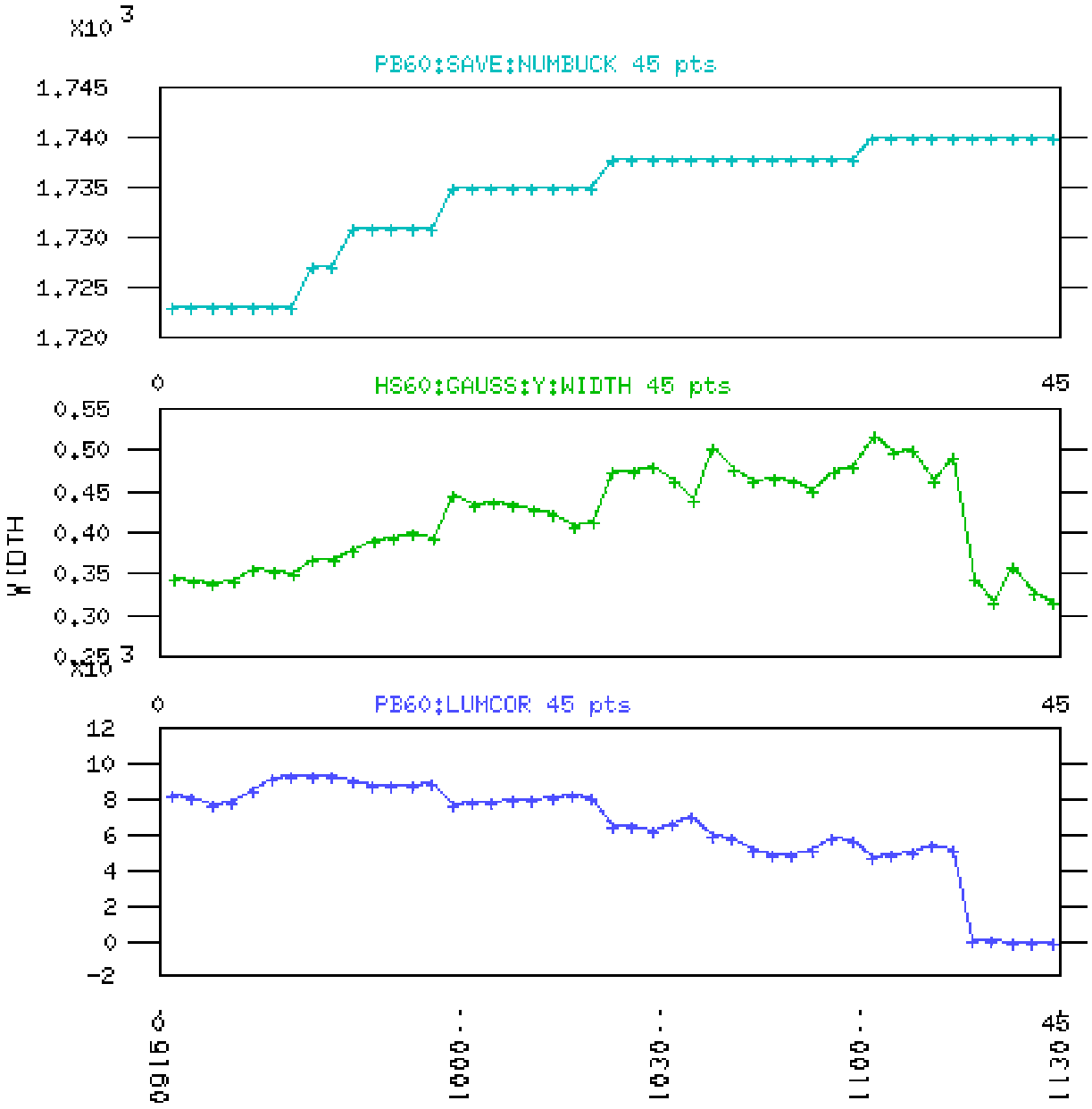
X10 3
PB60:SAVE:NUMBUCK 45 pts
1.745
1.740
1.735
1.730
1.725
1.720
0
45
HS60:GAUSS:Y:WIDTH 45 pts
WIDTH
0.55
0.50
0.45
0.40
0.35
0.30
0.25
X10 3
0
45
PB60:LUMCOR 45 pts
12
10
8
6
4
2
0
-2
0 9160
1000 - 1030 - 1100 - 45 1130

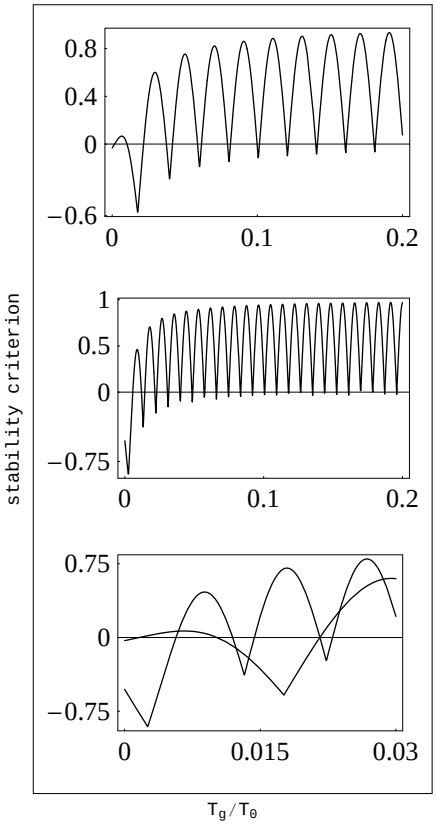

Figure 9: Multi-turn criterion of stability in x-plane (top) and y-plane (middle). The bottom pane shows zooming for both planes. Positive values correspond to unstable ions. For large gaps, almost all ions are unstable. For the gaps $T_g/T_0 < 0.002$ and $0.012 < T_g/T_0 < 0.0143$, ions are stable in both planes. Note that stability first starts in x-plane.

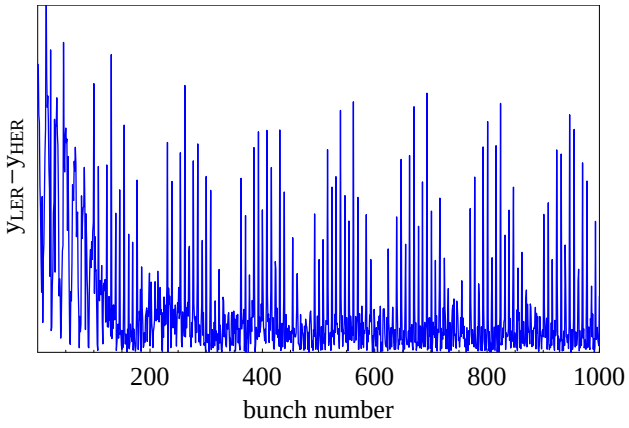

Figure 10: Relative offset of colliding beams modulated with the ion- and electron-frequencies. Result may be relevant for understanding the pattern of instability along the train.

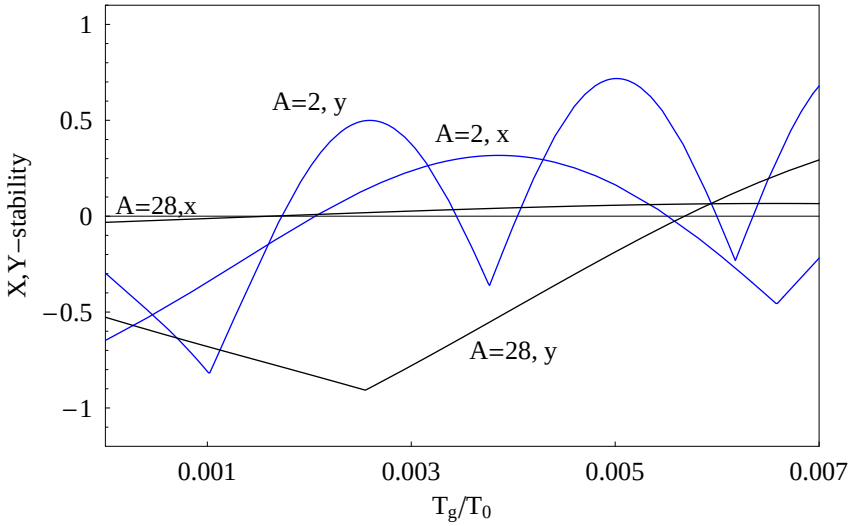

Figure 11: Comparison of the ion stability at small gaps for two species with atomic numbers $A = 2$ and $A = 28$. Heavier ions stay stable for larger gaps.

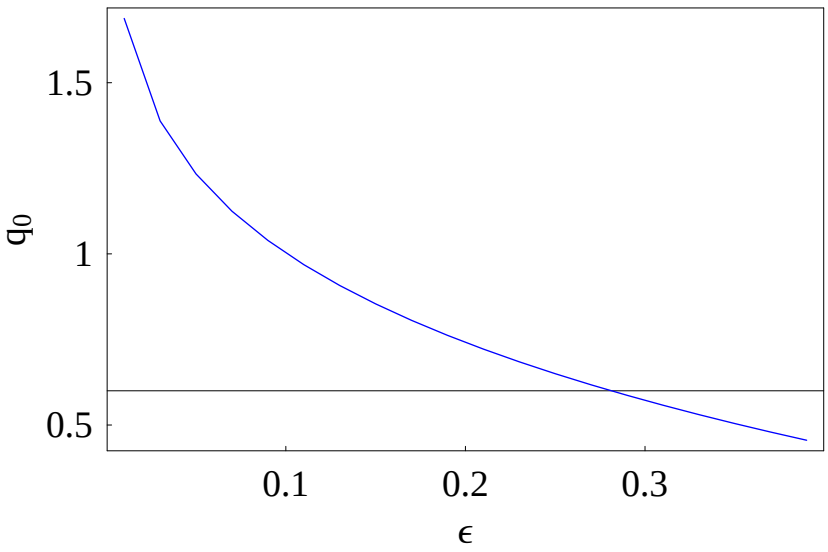

Figure 12: The root of Eq. (75) vs ϵ.